Experimental Evidence for Detuning Induced Pattern Selection in Nonlinear Optics

U. Bortolozzo and P. Villoresi*
DEI–Università degli Studi di Padova and Istituto Nazionale per la Fisica della Materia, Padova, Italy
P. L. Ramazza
Istituto Nazionale di Ottica Applicata, Florence, Italy
(Received 4 August 2000; revised manuscript received 3 July 2001; published 13 December 2001)

We give quantitative experimental evidence of the influence of cavity detuning in determining the pattern selection in a one-dimensional large Fresnel number optical oscillator. The issues of the selection of the transverse mode close to threshold and the value of the pump parameter at threshold are addressed. Competition between right and left traveling waves, resulting in a winner takes all dynamics, is also reported. Experimental results are in quantitative agreement with the theoretical predictions formulated for a broad class of systems comparable to the one here considered.

DOI: 10.1103/PhysRevLett.87.274102 PACS numbers: 42.65.Sf, 47.54.+r

Transverse structuration of light beams is a phenomenon common to many physical systems and devices in which radiation is coupled to some nonlinear optical material [1]. A role of central importance in this class of nonlinear optical systems is played by optical oscillators, among which lasers and optical parametric oscillators (OPO's) have been the most extensively studied and technologically implemented. For several of these oscillators, a common mechanism of pattern selection at threshold, based on the balance between cavity detuning and angular tilt of the selected wave with respect to the device optical axis, have been theoretically identified [2–5]. The same mechanism has been predicted to occur in passive optical systems as well [6]. In this paper we present an experimental study of the detuning induced transverse mode selection and of the corresponding variation of the oscillation threshold in an optical oscillator with gain provided by a photorefractive crystal. Close analogies have been established between photorefractive oscillators and lasers [7] or OPO's [5], depending on the pumping geometry.

Previous experimental works have reported the qualitative dependence on cavity detuning of the transverse pattern selected in photorefractive oscillators [8–10] or in vertical cavity surface emitting semiconductor lasers (VCSEL's) [11]. Using a VCSEL device, the quantitative dependence of the pattern scale on the tuning have been recently measured [12]. To the best of our knowledge, however, a full quantitative confirmation of the theoretical predictions about this phenomenon is not yet available.

Our experimental setup is shown in Fig. 1. It consists of a linear optical cavity formed by two end mirrors $R1$ and $R2$ and two confocal lenses L of focal length $f = 141$ mm, situated, respectively, at distances $f + l$ and f from the mrrors, the length $l = 5$ mm. The mirror reflectivities are 99% for $R1$ and 90% for $R2$. Mirror $R1$ is mounted on a piezo stack PZ interfaced to a PC, allowing fine control of the cavity length. A slit SL of 0.12 mm width placed in front of $R2$ allows the oscillation of cavity field in a plane, thus avoiding the possible occurrence of several secondary instabilities proper of the two-dimensional case, theoretically predicted in the context of laser equations [3] and already observed in similar experiments [8,11,12]. The active medium is a $5 \times 5 \times 5$ mm^3 $BaTiO_3$ crystal C, placed in the common focal plane of the two lenses, which is pumped by a single longitudinal and transverse mode Ar^+ laser. Videocameras $V1$ and $V2$ visualize, respectively, the planes of slit and of the crystal. Photodiode PD measures the oscillating signal spatially integrated intensity.

Let us examine the transverse mode selection imposed by our cavity. In the limit case $l = 0$, it is known that any transverse field distribution is an eigensolution of the propagation problem [13]. The introduction of $l \neq 0$ lifts this high degree of degeneracy, leaving as cavity modes only those field distributions that are plane waves in the regions between each mirror and its nearest lens and spherical waves in the region between the two lenses, where the crystal is located.

The relevant dynamical variables of the system are the electric field $\tilde{E}$ oscillating in the resonator, and the nonlinear refractive index $\tilde{n}$ of the photorefractive crystal. Using x as transverse coordinate, we describe the evolution of the system by means of the coupled equations:

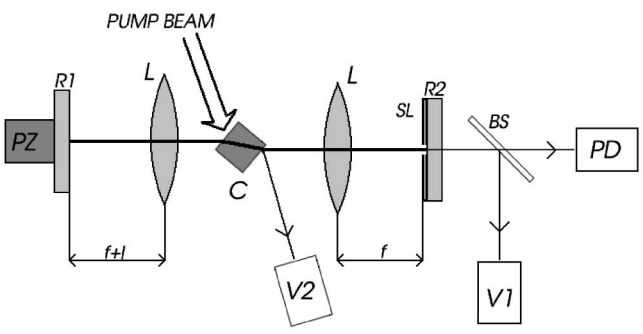

FIG. 1. Schematic diagram of the experimental setup.

$$\frac{\partial E(x,t)}{\partial t} = -\kappa E(x,t) + ia\frac{\partial^2 E(x,t)}{\partial x^2} + igE_p n(x,t), \quad (1)$$

$$\frac{\partial n(x,t)}{\partial t} = -[\gamma + i\Omega]n(x,t) - i\beta\frac{E_p^* E(x,t)}{|E_p|^2 + |E(x,t)|^2}, \quad (2)$$

where E, n are the slowly varying amplitudes of $\tilde{E}$, $\tilde{n}$ around the carrier frequency ω_c and the detuning $\Omega = \omega_p - \omega_c$, respectively, ω_p and E_p are the frequency and amplitude of the pump field, ω_c is the frequency of the cavity longitudinal modes closest to ω_p, κ and γ are the cavity photon decay rate and the inverse of the photorefractive response time, $g = \frac{\omega_c}{n_0}$, n_0 is the unperturbed refractive index, and β is a constant that incorporates the dependence of the field-index coupling on the crystal and laser beam parameters and on the geometry of the interaction [14–16]. The parameter a in Eq. (1) weights the effect of diffraction. In the case of free light propagation in a lensless system, it would be $a = c/2k_0$, where c and k_0 are the velocity and longitudinal wave number of the propagating field. Since in our cavity, due to the presence of the pair of confocal lenses, diffraction is effective for a length $2l$ over a cavity round trip, the length of which is $2(4f + l)$, we have to keep $a = \frac{c}{2k_0}\frac{l}{(4f+l)}$.

Equations similar to (1) and (2) have been introduced for a photorefractive oscillator in [7]. As compared to the case there considered, we are here dealing with a crystal to which no external electric field is applied. As a consequence, the coupling constants g and β are purely real in our case. Exactly the same equations, with the addition of a third one for the population inversion, are used in the description of a two-level laser, and known in that context as Maxwell-Bloch equations [17–20].

Linear stability analysis of the "nonlasing solution" $E = n = 0$ of Eqs. (1) and (2) can be carried out following exactly what has been done in [2,3,20] for the Maxwell-Bloch case. The results of this analysis predicts the values of the coupling strength βg, critical transverse wave number q_c, and lasing frequency ω_l at the bifurcation threshold, and are summarized in Table I.

In writing these results we assumed $\kappa \gg \gamma$, which is true for a photorefractive oscillator since $\kappa \simeq 10^8$–10^9, $\gamma \simeq 10^{-1}$–10 depending on the total illumination upon the crystal. Until this approximation is not adopted, the results of linear stability analysis are strictly identical to those reported in [2,3,20] for a two-level laser. The basic result predicted is the qualitative and quantitative dependence of the bifurcated state on the sign of the detuning. Indeed, lasing on a homogeneous state is expected for $\Omega < 0$, in which case the oscillating field does not have the possibility to match the temporal frequency of the pump field by traveling at a finite angle with respect to the cavity axis; this also results in an increase of the lasing threshold for increasing $|\Omega|$. For $\Omega > 0$, on the contrary, the above sketched mechanism of frequency tuning by means of spatial tilting is possible, so that for any value of Ω the cavity field will start oscillating at the same threshold value, have the same temporal frequency as the pump, but have an Ω-dependent finite transverse wave number.

TABLE I. Results of linear stability analysis of the solution $E = n = 0$.

	$\Omega < 0$	$\Omega > 0$
Threshold	$(\beta g)_{\text{th}} = \kappa\gamma[1 + \frac{\Omega^2}{\kappa^2}]$	$(\beta g)_{\text{th}} = \kappa\gamma$
Critical wave number	$q_c = 0$	$q_c = \sqrt{\frac{\Omega}{a}}$
Lasing frequency	$\omega_l = \omega_p - \frac{\gamma}{\kappa}\Omega$	$\omega_l = \omega_p$

In order to compare the predictions of the theory with the experiment, we performed a series of measurement varying the cavity length by means of the piezo driven mirror $R1$, while keeping fixed all the other parameters. If we denote as l_0 a value of l for which the cavity resonates with the pump frequency, and Δl the variation $l - l_0$ induced by the piezo, it follows that the pump-cavity frequency detuning is given by $\Omega = \omega_p \frac{\Delta l}{4f + l_0}$.

A first, rough scan of the cavity length showed that, when Δl is progressively increased, the field observed on the slit changes periodically from homogeneous to patterned at low spatial frequencies, to patterned at higher spatial frequencies, till eventually switching off and then restarting from the homogeneous state. This is in qualitative agreement with the previously described scenario of pattern selection, and allows us to identify regions of negative and positive cavity detuning with respect to a certain longitudinal mode. For one of these modes then we set the piezo so that $\Omega < 0$, and measure the beating frequency $\omega_p - \omega_l$ between the oscillating and pump field for a set of Ω values. Since $\omega_p - \omega_l \propto \Omega \propto \Delta l$, this measure allows us to define the position of the piezo at which the cavity is tuned with the pump. Then we scan the cavity length in a systematic way, letting the system evolve for about 1 min after each variation of Ω. We actually observe homogeneous states for $\Omega < 0$ and patterned

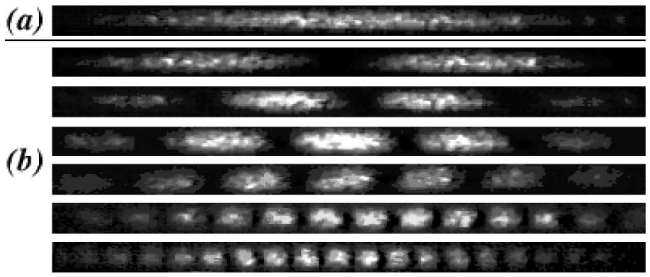

FIG. 2. Sequence of intensity pattern observed, through $V1$, when the detuning is negative (a) ($\Omega = -110$ MHz) and positive (b). In particular, (b) show the patterns, before the competition, from low (upper picture) to high Ω (370 MHz for the lower picture).

states for $\Omega > 0$, as shown in Fig. 2. There is a further difference between the two cases, however. While for $\Omega < 0$ the pattern readjusts itself in a few seconds after each parameter variation and then remains stable, the same is not true for $\Omega > 0$. In this case any of the cavity length variations are followed by the formation of a standing wave at a new wave number, still in the course of some seconds. After this, on a slightly longer time scale, we observe competition between the right and left traveling waves, resulting finally in the survival of only one of the two at the expenses of the other. It follows that in the final state the light distribution on the slit is homogeneous. Pictures displaying the time evolution of the field observed are shown in Fig. 3.

This competition phenomenon was predicted in [2,3] in the context of a two-level laser model, and is there to explain in terms of the fact that, in the interaction between the two traveling waves, cross saturation is prevalent over self-saturation. The winner takes all dynamics here observed arises under rather general conditions, and is similar to the one previously reported in other optical systems [21,22].

The time scales involved in the experiment are as follows: the pattern dynamics occurs over seconds; hence it is much longer than the piezo-induced cavity length variations, which occur in the milliseconds scale. The possibly dangerous time scale is that of unwanted cavity length variations due to environmental fluctuations. This typical time was measured by standard interferometric technique to be of the order of tens of minutes in the best conditions that we then used for the measurements.

Use of the previously described procedure to set the tuning point of the cavity before each complete set of measurements, which takes a few minutes, ensures stability and reproducibility of the experiment even without the use of an active stabilization loop for the cavity length. In a range of Ω of the order of 200 MHz around $\Omega = 0$, however, the observed situation is less clear than reported above and irregular jump between homogeneous and patterned states is sometimes observed. This is compatible with the fact that in this region the two states have similar thresholds. We believe that the present stability of our experimental setup does not allow a reliable study of the dynamics in this regime, hence we do not report measurement relative to a region of Ω around the origin.

We measured the dependence of the bifurcating wave number q_c as a function of detuning in the case $\Omega > 0$. The measurement was performed by taking images in the plane of mirror $R2$ at the time instant for which the standing wave is observed at its maximum intensity. The results are shown in Fig. 4, and display good agreement with the predictions of the linear stability analysis. In particular, the scaling law $q_c \propto \sqrt{\Omega}$ is verified.

By solving Eqs. (1) and (2) at equilibrium and using the approximation $1/(|E|^2 + |E_p|^2) \simeq \frac{1}{|E_p|^2}(1 - \frac{|E|^2}{|E_p|^2})$, valid for $|E| \ll |E_p|$, we obtain

$$\frac{\beta g_{\text{th}}}{\beta g} = 1 - \frac{|E|^2}{|E_p|^2}. \tag{3}$$

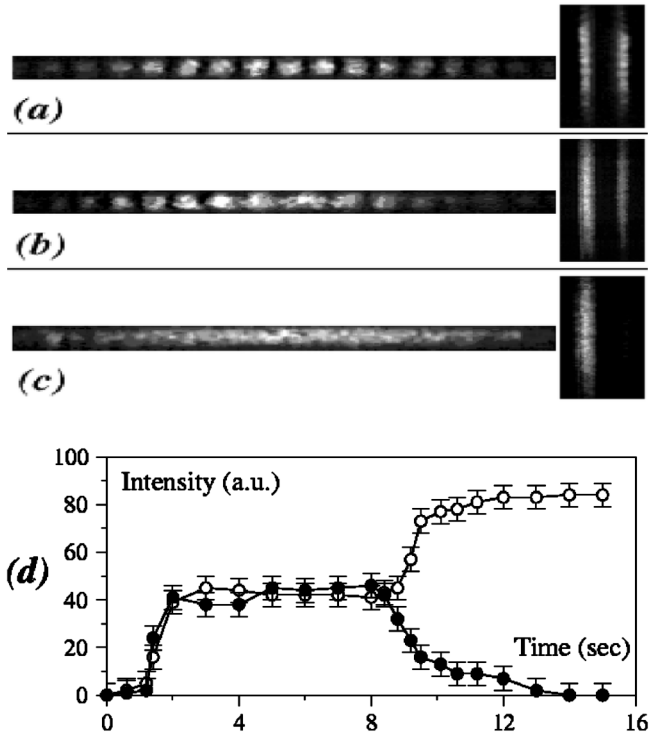

FIG. 3. (a)–(c) Temporal sequence of patterns observed in the plane of $R2$ (left pictures) and of the crystal (right pictures) for positive detuning. The pictures show the following: (a) the formation of a standing wave; (b) and (c) the competition between the right and the left traveling waves and the survival of only one traveling wave; (d) the time evolution of the power for the right and left traveling waves.

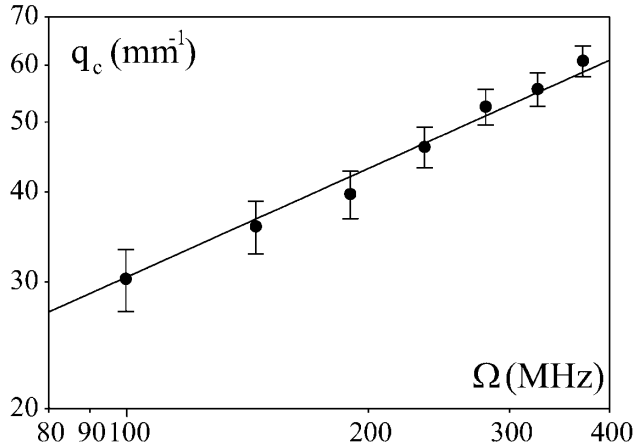

FIG. 4. Dependence of selected wave number q_c on cavity detuning Ω measured for $\Omega > 0$, in log scale. Dots: experiment; line: plot of $q_c = \sqrt{\frac{\Omega}{a}}$. a, Ω are evaluated using their definitions and the experimental parameter values given in the text.

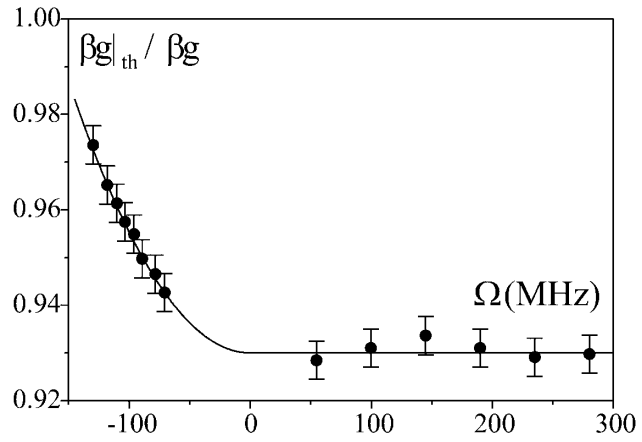

FIG. 5. Normalized threshold coupling as a function of cavity detuning. Dots: experiment; line: fit of the data with a parabola for $\Omega < 0$, a constant for $\Omega > 0$. See text for details on the fit function and parameters.

Equation (3) allows us to evaluate the normalized threshold coupling parameter $\frac{\beta g_{\text{th}}}{\beta g}$ from measurements of $|E|^2$ and $|E_p|^2$. For this purpose the value of the oscillating intensity $|E|^2$ is measured, for each value of cavity length, after the transient regime in which competition between right and left traveling waves is terminated.

The behavior of $\frac{\beta g_{\text{th}}}{\beta g}$ as a function of cavity detuning is shown in Fig. 5.

As expected, the threshold is constant for positive detuning, while it increases parabolically for negative detuning. Following the results of the linear stability analysis reported in Table I, the parabola used in order to estimate the value of κ from the experimental data at $\Omega < 0$ is

$$\left.\frac{\beta g_{\text{th}}}{\beta g}\right|_{\Omega<0} = \left.\frac{\beta g_{\text{th}}}{\beta g}\right|_{\Omega>0} \left(1 + \frac{\Omega^2}{\kappa^2}\right). \qquad (4)$$

The result $\kappa = 6.06 \times 10^8\ \text{s}^{-1}$ is used to draw the solid line in Fig. 5, and is within 10% of the value calculated for this parameter taking into account the cavity losses measured in the experiment. In conclusion, our results confirm quantitatively the predictions about the selected transverse pattern and the oscillation threshold on cavity detuning.

The authors thank Professor F. T. Arecchi for revising the text and Professor G. Tondello for the support he provided.

*Email address: Paolo.Villoresi@dei.unipd.it

[1] For recent reviews about this topics, see, e.g., special issue on *Pattern Formation in Nonlinear Optical Systems,* edited by R. Neubecker and T. Tschudi [Chaos Solitons Fractals **10**, No. 4/5 (1999)]; F. T. Arecchi, S. Boccaletti, and P. L. Ramazza, Phys. Rep. **318**, 1 (1999); special issue on *Patterns in Nonlinear Optical Systems,* edited by W. Lange and T. Ackemann [J. Opt. B **2**, No. 3 (2000)].
[2] P. K. Jacobsen, J. V. Moloney, A. C. Newell, and R. Indik, Phys. Rev. A **45**, 8129 (1992).
[3] P. K. Jacobsen, J. Lega, Q. Feng, M. Staley, J. V. Moloney, and A. C. Newell, Phys. Rev. A **49**, 4189 (1994); **49**, 4201 (1994).
[4] G. L. Oppo, M. Brambilla, and L. A. Lugiato, Phys. Rev. A **49**, 2028 (1994).
[5] G. J. de Valcarcel, K. Staliunas, E. Roldan, and V. J. Sanchez-Morcillo, Phys. Rev. A **54**, 1609 (1996).
[6] W. J. Firth and A. J. Scroggie, Europhys. Lett. **26**, 521 (1994).
[7] K. Staliunas, M. F. Tarroja, G. Slekys, C. O. Weiss, and L. Dambly, Phys. Rev. A **51**, 4140 (1995).
[8] K. Staliunas, G. Slekys, and C. O. Weiss, Phys. Rev. Lett. **79**, 2658 (1997).
[9] A. V. Mamaev and M. Saffman, Opt. Commun. **128**, 281 (1996).
[10] V. B. Taranenko, K. Staliunas, and C. O. Weiss, Phys. Rev. Lett. **81**, 2236 (1998).
[11] S. P. Hegarty, G. Huyet, J. G. McInerney, and K. D. Choquette, Phys. Rev. Lett. **82**, 1434 (1999); S. P. Hegarty *et al.,* J. Opt. Soc. Am. B **16**, 2060 (1999).
[12] T. Ackemann *et al.,* Opt. Lett. **25**, 814 (2000).
[13] J. A. Arnaud, Appl. Opt. **8**, 189 (1969).
[14] A. Yariv and S. Kwong, Opt. Lett. **10**, 454 (1985).
[15] *Photorefractive Materials and Their Applications,* edited by P. Gunter and J. P. Huignard (Springer-Verlag, Berlin, 1988).
[16] Ph. Refregier, L. Solymar, H. Raijbenbach, and J. P. Huignard, J. Appl. Phys. **58**, 45 (1985).
[17] F. T. Arecchi, G. Lippi, G. P. Puccioni, and J. R. Tredicce, Opt. Commun. **51**, 308 (1984).
[18] L. A. Lugiato, C. Oldano, and L. M. Narducci, J. Opt. Soc. Am. B **5**, 879 (1988).
[19] P. Coullet, L. Gil, and F. Rocca, Opt. Commun. **73**, 403 (1989).
[20] A. C. Newell and J. V. Moloney, *Nonlinear Optics* (Addison-Wesley, Redwood City, CA, 1992).
[21] C. Benckert and D. Z. Anderson, Phys. Rev. A **44**, 4633 (1991).
[22] M. A. Vorontsov and W. J. Firth, Phys. Rev. A **49**, 2891 (1994).